RC 20773 (02/14/97)
Computer Science 24 pages

IBM Research Report

Using Scout Images to Reduce Metal Artifacts in CT with Application to Revision Total Hip Surgery

Alan D. Kalvin

IBM Research Division
T.J. Watson Research Center
Yorktown Heights, New York
kalvin@watson.ibm.com

Bill Williamson

Integrated Surgical Systems
829 West Stadium Lane
Sacramento, CA 95834
billw@calweb.com

IBM Research Division
Almaden · T.J. Watson · Tokyo · Zurich

Using Scout Images to Reduce Metal Artifacts in CT with Application to Revision Total Hip Surgery

ABSTRACT

X-ray CT images of objects containing metal are often corrupted by "blooming" and streaking artifacts that radiate from the regions of the image where the metal is present. The ideal strategy for reducing these artifacts is to modify the noisy projection data (sinogram data) before reconstructing the image. Unfortunately this approach does not lead to a very practical solution, since it assumes that one has access to the unencoded projection data. In reality, these data are virtually impossible to get, even for isolated research studies, let alone for routine clinical use.

Our goal is to produce a practical, clinically useful system for reducing metal artifacts in real patient CT scans on a regular basis. Therefore we want a method that does not depend on sinogram data. However, it is extremely difficult, if not impossible, to reduce metal artifacts using just the information than exists in the noisy CT image itself. As we show, crucial image details may be completely erased by the artifacts. Therefore we have developed a new approach for suppressing these reconstruction artifacts by using a small number of scout images. We have applied this method successfully to real CT data.

Keywords: CT artifacts, scout images, reconstruction from projection, revision total hip replacement.

This work was performed with the support of the U.S. Department of Commerce, National Institute of Standards and Technology.

1 INTRODUCTION

X-ray CT images of objects containing metal are often corrupted by "blooming" and streaking artifacts that radiate from the regions of the image where the metal is present (Figure 1). The focus of this work is the development of a method to reduce metal-induced reconstruction artifacts in CT images. In particular we are concerned with CT images used in surgical planning of revision total hip replacement (RTHR). This work is part of a on-going project to extend the Integrated Surgical Systems ROBODOC™system for primary total hip replacement (PTHR) to RTHR. A major challenge here is to provide the surgeon a way to plan surgery from noisy CT images of patients who have large metal prostheses implanted in their femurs.

Metal-induced reconstruction artifacts (from now on we will refer to simply as metal artifacts) in CT scans of RTHR patients are most marked in CT images of the proximal femoral section, where the implant is the thickest. The artifacts make it difficult to determine the boundary between the implant, the cement, and the bone. Since the quality of the CT images is key in determining the quality of the surgical plan, reducing these artifacts as much as possible is essential.

A number of approaches have been previously considered for reducing metal artifacts in CT images. These include (1) using implants made of materials with lower attenuation coefficients, or with smaller cross-sectional areas [11]; (2) using higher energy X-rays beams that will not be blocked by the implants [11]; (3) applying image processing methods to directly to the noisy CT images [11, 13, 14]; (4) averaging out the effect of the artifacts by combining multiple image sets, each scanned with the gantry at a different angle [12, 16]; (5) processing the projection data directly (typically by filling in "missing" data), and then reconstructing the images from these modified projections [2, 4, 5, 6, 7, 8, 9, 15].

For reducing artifacts in CT images of RTHR patients, (1) is obviously not an option. The need for limited patient dose and low energy to discriminate among materials (including both biological tissue types, and synthetic material like cement) rules out (2). Approach (3) is limited by the fact that essential image information may be completely erased by the artifacts, and this information cannot be recovered solely from the corrupted images themselves. Technique (4) requires longer scanning time and higher patient exposure to radiation.

In principle approach (5) can produce the best results. Since metal artifacts arise from reconstructing images from corrupted projections, the best possible way to reduce the artifacts is to modify the projections before they are used in the reconstruction process. However it is impractical to develop an artifact reduction system for clinical use that depends on the CT sinogram data. Our experience (which seems typical of other researchers in this area) is that it is extremely difficult to get access to unencoded sinogram data even for a single research study, let alone on a regular basis for routine patient scans. Therefore artifact reduction methods that rely on access to these data are of limited practical use.

Since it is essential for us to have a method that is clinically viable, we have developed a new approach to artifact reduction, based on the use of scout images.

2 SCOUT IMAGES AS PROJECTION DATA

CT scout images are a form of unencoded projection data that are readily available to users of standard clinical CT scanners. With a typical hospital CT scanner, a set of projection data is produced by keeping the table stationary while the x-ray tubes rotates around the patient. Data are collected at fixed positions of the x-ray tube. A complete set of these data is called a *sinogram*, and is used to reconstruct one 2D image.

CT scanners can also produce x-rays known as *scout images*. A scout image is produced by keeping the x-ray tube in a fixed position and moving the table. Scout data, unlike sinogram data, are easy to get in unencoded form during routine patient scanning. Figure 2 shows a scout image of an RTHR phantom that we designed for this study. The phantom consists of a cadaver femur with an implanted metal prosthesis, lying inside a water-tank[1]. Alongside this phantom in the figure is a standard thigh phantom.

Figures 3 and 4 shows the relationship between scouts images and sinogram data. A set of scout images, which was acquired sequentially by moving the x-ray tube around the patient, is shown stacked into a 3D volume in Figure 3. Figure 4 shows this 3D volume sliced in the "Table Position" dimension, that is, each slice corresponds to the set of data acquired at all x-ray tube positions, and at a fixed table position. This is of course equivalent to a sinogram, and the typical sinusoidal-like patterns that give a sinogram its name are can be easily seen.

The basic difference between acquiring sinogram data and scout data is the order in which the table and the x-ray tube are move. Therefore in principle we can use scout data instead of sinogram data to reduce metal artifacts. In practice though there are a number of issues that need to be considered. Both scout and sinogram data are derived from processing the same set of raw projection data, but the process is quite

[1]See section 5 for more details about the phantom and the scanning protocol we used.

different in each case. Scout images are designed for visually planning CT scanning sessions, and they are not as well-suited for image reconstruction as sinogram data. This means that images reconstructed from scouts will be of poorer quality than those reconstructed from sinograms.

To determine the feasibility of basing an artifact reduction method on the use of scouts, we first investigated whether it was possible at all to accurately reconstruct CT images from scouts. Initially we experimented using a large (and clinically prohibitive) number of scouts.

3 IMAGE RECONSTRUCTION FROM SCOUT DATA

After scanning the phantom shown in Figure 2 (a), we re-sliced the 3D volume of scout data into a set of sinogram-like projection data, and reconstructed the CT images using a standard filtered back-projection method [10]. Figure 5 shows a slice from this reconstruction (a), and the corresponding original CT image (b).

As these results show, it is indeed possible to reconstruction CT images from scouts data. Therefore we could, in principle at least, apply artifact reduction algorithms that require projection data [2, 4, 5, 6, 7, 8, 9, 15]. to these data, in the place of the true sinogram data.

Unfortunately, this would require more scouts than is clinically acceptable (both in terms of scanning time, radiation dosage). On the other hand, reconstructions from a small, and tolerable, number of scout images gives unacceptably poor results. Figure 6 shows the result of reconstructing from 12 scouts using standard filtered back-projection and algebraic reconstruction(ART)[3] algorithms.

4 ARTIFACT REDUCTION WITH A SMALL NUMBER OF SCOUT IMAGES

Since reconstructing satisfactory images from scout data requires a prohibitive number of scouts, we have developed MARCUS[2], a new algorithm for reducing metal artifacts in CT images that uses just a small (and clinically acceptable) number of scouts.

[2]Metal Artifact Reduction Using Scouts.

Being limited to using a few scouts, rather than a full set of sinograms, greatly restricted our choices in designing the algorithm. Therefore we developed our method based on the following criteria:

1. We need to reduce the effects of artifacts in a local area of the image only, rather than over the whole image. That is, we need only restore details in the region around the metal implant only[3].

2. We are mainly interested in recovering boundaries between objects, rather than recovering absolute pixel densities.

3. We can run the method off-line, so we need not be overly concerned with speed. We are not designing a method that has to run in real-time as part of a CT scanner's reconstruction algorithm.

MARCUS is an iterative algorithm that reduces the metal artifacts by repeatedly modifying the corrupted CT image by applying two sets of constraints:

1. **Image constraints** that are based on information about of the objects in the image.

2. **Projection constraints** that are constraints imposed by the scout data.

The algorithm works as follows. First the image is updated according to the image constraints. Then this modified image is checked against the scout data, and it is adjusted to reduce the degree of inconsistency between the two. This two-step iterative process is repeated until the desired termination criteria have been met. Typically criteria for termination are (a) the change in the image between successive iterations falls below a threshold, or (b) the maximum number of iterations has been reached.

Note that although we have designed the method for use with scout data, it is completely general in the sense that it is applicable to any set of projection data.

4.1 Computing image constraints

To compute image constraints we consider two classes of objects in the the artifact-corrupted CT image: (I) *clear* objects; and (II) *fuzzy* objects.

Clear objects are those whose exact boundaries in the image are clear, and readily discernable. Examples of clear objects are:

[3]Unfortunately, this is the area of the image that suffers most from the artifacts.

- *Intrinsic scene* objects, like the CT scanner table and the aluminum motion-detection rod used in RTHR scans, that are regular elements of the scene being scanned;

- *Extrinsic scene objects*, which are inserted into the scene being scanned specifically to create additional image and projections constraints.

- Regions of patient anatomy that show up sharply in CT images;

Fuzzy objects are objects that are easily identifiable-in the image, but whose boundaries are unclear because of reconstruction artifacts. Examples of fuzzy objects are:

- metal hip implants,

- bone-cement (used to secure implants), and

- other objects on the vicinity of implants.

Since a clear object has well-defined boundaries, we can identify the set of pixels representing it in the image. The object's correct density values, or range of values, defines a set of constraints that are satisifed by simply updating the appropriate pixels.

The fuzzy object that is of most interest to us is the metal implant. Since we cannot locate the precise boundary of the implant in the image, we cannot update the image pixels as we do for clear objects. We can however, use the scout data to define bounds on where the implant border can be, using the basic property of the Radon transform [1] that each point in projection space corresponds to a line in image space.

While the boundaries of a fuzzy object cannot be clearly identified in the image, we can use the scout data to identify lines that are tangent to this boundary. For metal objects these tangent lines correspond to sharp edges in the scout images. Given an edge in the scout image and the CT scanner geometry, it is easy to find the tangent line in the CT image corresponding to the edge. Figure 7 gives an example, taken from real CT data. Part (a) shows a scout image of our cadaver phantom with a pair of edges in the first column highlighted. These are the edges of the aluminum bone-motion rod that is used scanning ROBODOC™patients. Part (b) shows the corresponding pair of tangent lines in the CT image computed from the edge data.

Figure 8 illustrates how we can determine limits on the boundary of a fuzzy object. Figure 8 (a) shows an elliptical object and 4 pairs of lines that are tangent it. Assuming that all we know about the shape of the object is that its boundary touches all 8 tangents. It is quite easy to show that from this information we can partition the image pixels into three classes [4]:

1. *definitely inside* the object (the black polygonal area in Figure 8);

2. *possibly inside* the object (the grey area); and

3. *definitely outside* the object (everything else).

Based on this partitioning we can adjust the pixels values in classes (1) and (3) in the same way that pixels of clear objects are updated.

To check the consistency between the (now modified) image and the scout data, we note that each scout pixel represents the x-ray attenuation sum along a projection ray. For each ray, we compute the sum of the densities along the corresponding ray in the image. We then reduce the amount of inconsistency between the two sums by updating all the image pixels lying on the path of the ray.

This is, of course, the basic update process used in algebraic reconstruction techniques (ART)[3] for image reconstruction from projections. However here we are using it for artifact reduction rather than for reconstruction from projections. (As we have seen in Figure 6 using ART to reconstruct with a small number of scouts produces very poor results).

5 EXPERIMENTAL RESULTS

We have tested MARCUS on a realistic custom-built RTHR phantom which consists of a cadaver femur, a metal hip prothesis, and bone-cement. The femur was prepared by milling the femoral canal into a wider cavity and filling it with with polymethyl methacrylate (PPMA) bone-cement. Once the cement had hardened, the ROBODOC™system was used to cut a high-precision implant cavity in the bone-cement, providing a flush fit for the femoral implant (a stainless-steel Depuy AML

[4]Note that this method applies to convex shapes (like implant cross-sections), and to the convex hulls of non-convex shapes.

13.5 standard)[5].

This phantom mimics the femur of an RTHR patient, with the prothesis embedded in a mantle of bone-cement. For scanning, the phantom was clamped inside a radiolucent water-tank, and an aluminum motion-detection rod (that is used in standard ROBODOC™CT scans) fixed diagonally across the top of the tank.

The phantom was scanned at the Sutter Memorial Hospital, Sacramento using a GE CT Hilight Advantage scanner, with standard protocols for PTHR patients. We acquired two sets of scans, the first with the implant inserted in the femur, and the second set, scanned without the implant. The second set served as the ground-truth, since the precise milling of the implant cavity means that the cavity (which can be clearly see in the second set of scans), and the implant share a common boundary. To make sure that these two datasets were registered, we took particular care to prevent the phantom from moving while the implant was removed before the taking the second set of scans[6]

Figure 9 shows a pair of slices from these scans. On the left is the phantom with the metal implant (and clearly visible metal artifacts), and on the right, the phantom with no implant.

These scans provided us with a very useful data set, both for testing our method, and also for studying the characteristics on metal artifacts produced by femoral implants. We implemented MARCUS using IBM Visualization Data Explorer scientific visualization system, and a locally-modified version of the SNARK93 image reconstruction system [10].

For our first experiments we used the very simple intrinsic image constraint of setting the background to zero. We ran MARCUS using 12 scouts acquired with the x-ray tube positioned at 12 equally-spaced points around the table. Figure 10 shows the area around the femur in the original CT, and the results of running MARCUS for 50 iterations. The reduction of artifacts, and the recovery of details of the metal/bone-cement interface are quite noticeable.

[5]Stainless-steel implants produce metal artifacts that are far worse than those produced by any other type of metal implant (e.g. cobalt-chrome, titanium). Therefore the data we are working with represent an extreme worst-case situation.

[6]To confirm that the CT scans were registered, we checked at the absolute difference between pair of slices. We found that the only significant difference between each pair (besides the implant and artifacts, of course) was a slight drop in the water level in the second set caused by water filling the implant cavity. By having fixed the aluminum rod diagonally across the top of the tank, we were able to confirm registration in the direction of table travel too, using the horizontal position of the rod in each image.

The corresponding graphs in Figures 11 and 12 confirm these results. In both these graphs, the upper plot (marked with small circles at the vertices) is the density profile alone the line through the implant and bone-cement shown in Figures 10 (a) and (b). The lower plot (identical in both graphs) is the density profile along the same line for the corresponding CT scan with no implant (Figure 9 (b)). The pair of vertical lines at 12.6 mm. and 26.8 mm. in this lower plot indicates the true locations of the bone-cement/implant interface. From Figure 10 we can also see that:

1. In CT images like the ones shown here, crucial details in the regions close to metal objects do indeed get lost as a result of the "blooming" nature of the metal artifacts, and these details cannot be recovered from the corrupted image itself. The blooming is not (as one may suspect) simply the result of saturation at the high-end of the grey-scale map.

2. It is possible to recover the image details erased by metal artifacts using the additional information provided by a small (and clinically acceptable) number of scout images. As Figures 10 and 12 show, after running MARCUS, there are sharp, distinct edges at the bone-cement/metal-implant interface.

6 CURRENT AND FUTURE WORK

We are encouraged by the results that we have obtained with the simple image constraint of setting the image background to zero. We hope to get improved results by extending MARCUS to include the following features.

More advanced intrinsic and extrinsic constraints
We are currently experimenting with more elaborate intrinsic constraints, and we are working on introducing extrinsic constraints. Here we plan to (a) determine the kinds of objects that can provide effective extrinsic constraints, and (b) where to best position these objects relative to the patient during scanning.

Positioning of scouts
While we are limited to using a small number of patient scout images, we do have the freedom to choose which scouts we want. That is, we can choose where to position the x-ray tube when acquiring these scouts. (For example, the GE CT Hilight Advantage scanner allows scouts to be taken in tube increments of 1 degree, and the Siemens CT Somatom Plus 4 the tube position is selectable in 5 degree steps).

At present we have experimented only with tube positions equally spaced over 360 degrees. The next step is to evaluate the results obtained with other patterns of tube spacing.

Exploiting the 3D nature of the data

To convert scout data to sinogram-type data, we are forced to work with the data as a complete 3D volume. The positive side of this is that we can take advantage of having to work with 3D data to improve our results. For example, as we discussed in Section 4.1, we need to detect edges in scout data in order to compute constraints from fuzzy objects. It seems reasonable to assume that we will get better results running a 3D edge-detector the scout volume than we get running a 2D edge-detector on each scout image.

It is also possible to take advantage of the fact that the CT images form a 3D stack, and not to process each one in isolation. For instance, once artifact reduction has been applied to one 2D slice, we may be able to use the constraints and results obtained to speed-up and improve the processing of the following slices in the stack.

Testing MARCUS on real patient data

As we have stressed throughout this paper, our main goal is to produce a practical artifact reduction method that can be used successfully on real patients, in a regular clinical environment. While we have taken a lot of effort to acquire realistic test data, we won't know if our method is really any good clinically until we have tested it on real patients.

Running MARCUS with real sinogram data

There is nothing in the MARCUS system (besides in the name) that assumes that we are working with scout data, rather than another form of projection data. Even though it it not of practical use for RTHR, we plan to test MARCUS using true sinogram data to evaluate what improvements one can expect from working with better quality projection data.

7 CONCLUSION

We have considered the problem of metal artifact reduction in CT with particular focus on developing a practical method for revision hip surgery planning. We have discussed the reasons why a method that relies on projection (sinogram) data is not practical for routine patient use.

We have shown:

1. Metal artifacts can erase crucial image information, and this missing information cannot be recovered solely from the information in the noisy CT image itself.

2. It is possible to reconstruct CT images from scout data, but the number of scout images required to do this is not clinically acceptable.

3. It is possible to reduce CT metal artifacts and recover important image details by using a small number of scout images.

Finally, we have developed method that has worked successfully on CT data of a realistic, physical phantom containing a stainless-steel implant. Since the most severe metal artifacts are caused by stainless-steel, we expect our method to work as well, if not better, with implants made of other types of metal.

References

[1] S.R. Deans, *The Radon transform and some of its applications*, Krieger Publishing Company, Florida, 1993.

[2] G.H. Glover and N.J. Pelc, "An algorithm for the reduction of metal clip artifacts in CT reconstructions", *Medical Physics* 8(6), Nov/Dec 1981, pp. 799-807.

[3] G.T. Herman, *Image reconstructions from projections: The fundamentals of computerized tomography*, Academic Press, 1980.

[4] T. Hinderling, P. Ruegsegger, M. Anliker, C. Dietschi, "Computed tomography reconstruction from hollow projections: an application to in vivo evaluation of artificial hip joints", *Journal of Computer Assisted Tomography*, Feb 1979, 3 (1) pp. 52-57.

[5] W.A. Kalender, R. Hebel, and J. Ebersberger, "Reduction of CT artifacts caused by metallic implants." *Radiology*, Aug 1987, 164 (2) pp. 576-7.

[6] E. Klotz, W.A Kalender, R. Sokiranski, D. Felsenberg, "Algorithms for the reduction of CT artifacts caused by metallic implants." *Medical Imaging IV: PACS System Design and Evaluation*, Vol 1234, Newport Beach, CA, Feb 1990, pp. 642-650.

[7] R.M. Lewitt and R.H.T., Bates, "Image reconstruction from projections: IV: Projection completion methods (computational examples)", *Optik* 50, 1978, pp. 269-278.

[8] B.P. Medoff, "Image reconstructions from limited data: Theory and applications in computerized tomography", *Image Recovery: Theory and Application*, Henry Stark (ed), Academic Press, 1987.

[9] B.E. Oppenheim, "Reconstruction tomography from incomplete projections", *Reconstruction tomography in diagnostic and nuclear medicine*, Ter-Pogossian (editor), University Park Press, Baltimore, 1977, pp. 155-183.

[10] J. A. Browne, G.T. Herman, D. Odhner, *SNARK93: A programming system for image reconstruction from projections* Technical report MIPG198, Dept. of Radiology, University of Pennsylvania, August 1993. Mar-Apr 1988, 12 (2) pp. 236-41.

[11] D.D. Robertson, P.J. Weiss, E.K. Fishman, D. Magid, P.S. Walker, "Evaluation of CT techniques for reducing artifacts in the presence of metallic orthopedic implants", *Journal of Computer Assisted Tomography*, Mar-Apr 1988, 12 (2) pp. 236-41.

[12] C. Rozeik, O. Kotterer, J. Preiss, *et al.* , "Cranial CT artifacts and gantry angulation", *Journal of Computer Assisted Tomography*, May-Jun 1991, 15 (3) pp. 381-386.

[13] H. Soltanian-Zadeh, J.P. Windham, J. Soltanianzadeh "CT artifact correction: An image processing approach", *SPIE Medical Imaging 1996: Image Processing*, Vol 2710, 1996, pp. 477-458.

[14] H.K. Tuy, "Algorithm to reduce clip artifacts in CT images", *Medical Imaging VI: Image Processing Conference*, Newport Beach, CA Feb 1992, pp. 635-643.

[15] G. Wang, D.L Snyder, A. O'Sullivan, M.W. Vannier, "Iterative deblurring for CT metal artifact reduction", *IEEE Trans. Medical Imaging*, October 1996, 15 (5), pp. 657-664.

[16] B. Williamson, Unpublished note, Integrated Surgical Systems, 1994.

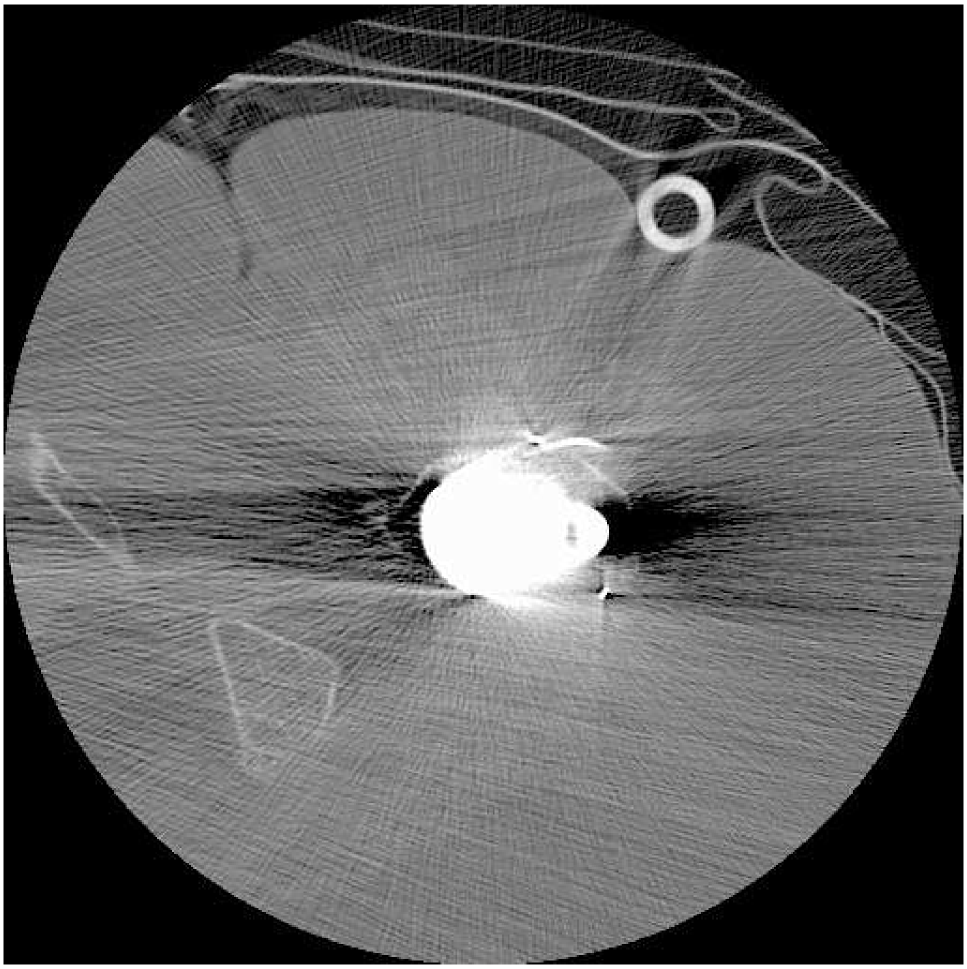

Figure 1: A CT image of a patient's femur with an implanted metal prosthesis.

Figure 2: A CT scout image.

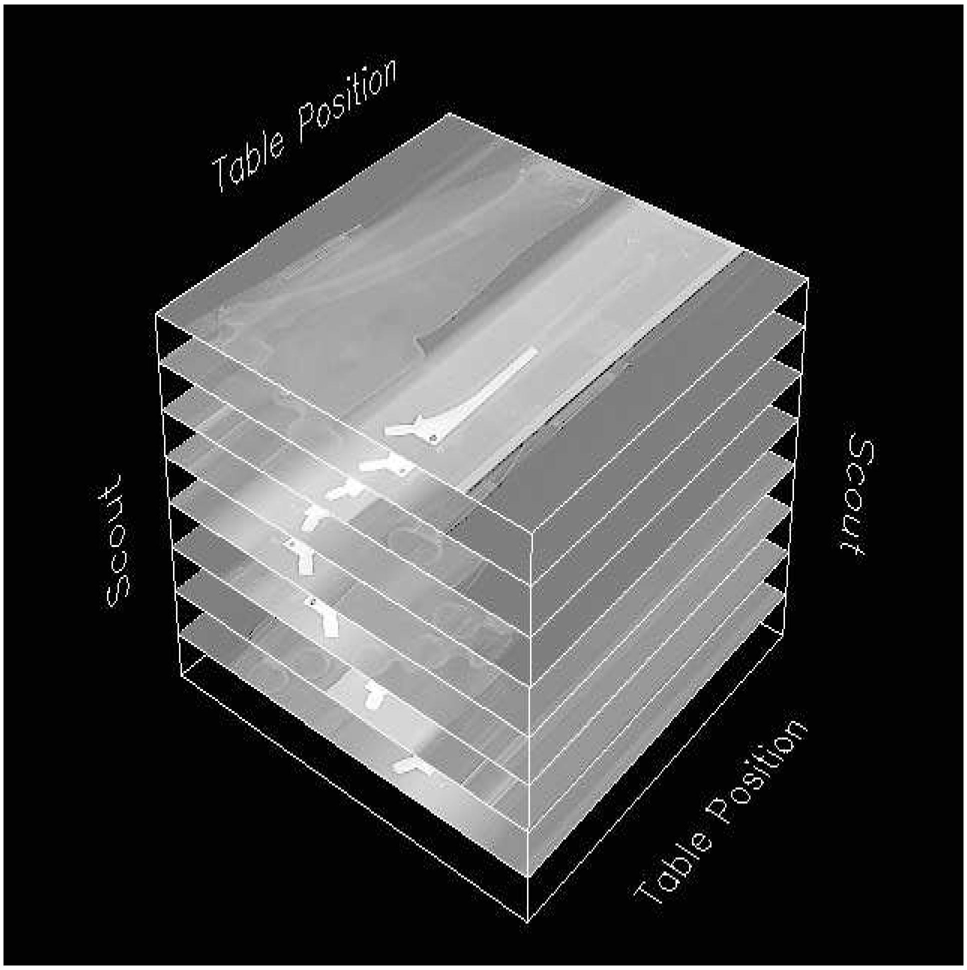

Figure 3: A stack of scout images.

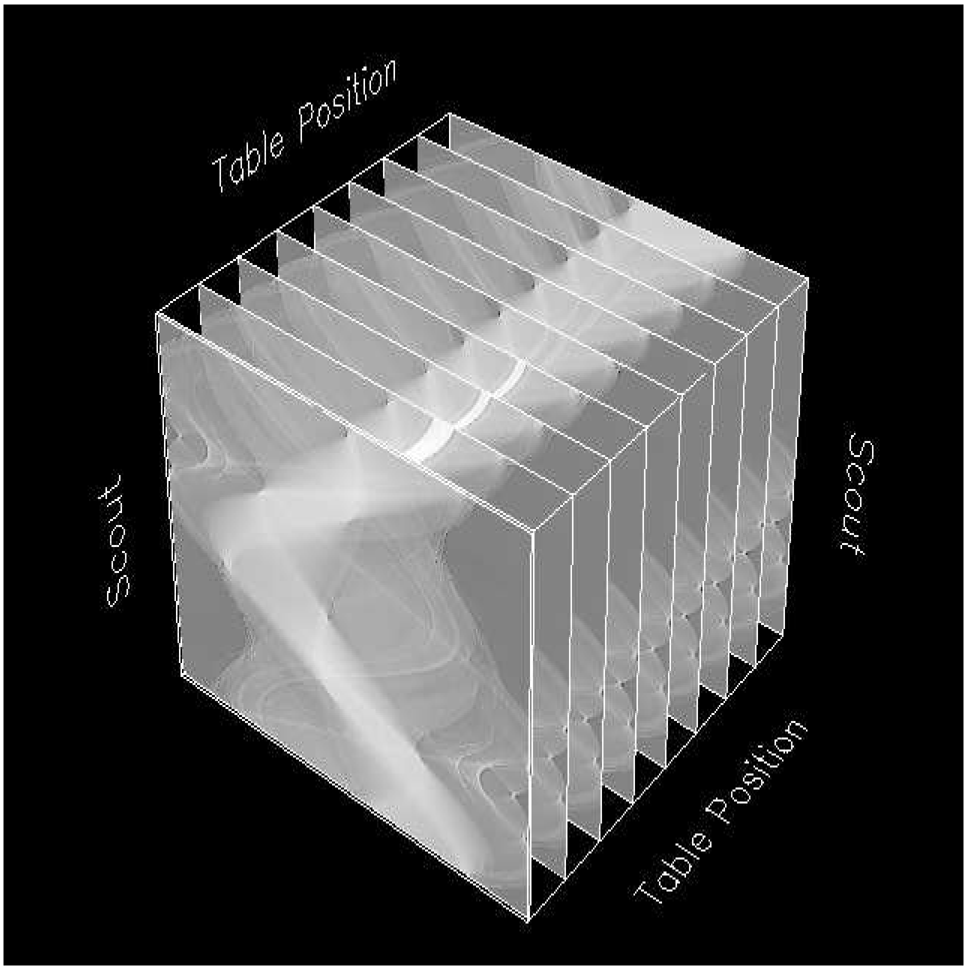

Figure 4: The scout images reformatted into a stack of sinograms-like projections.

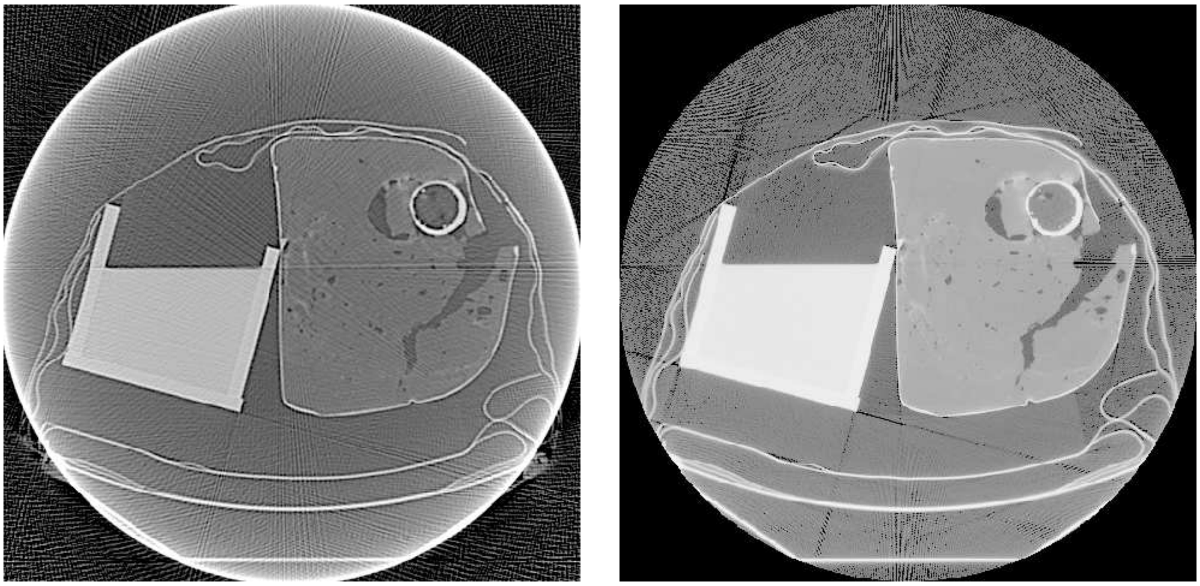

(a) (b)

Figure 5: (a) Filtered back-projection reconstruction from 360 scout images. (b) The original CT image.

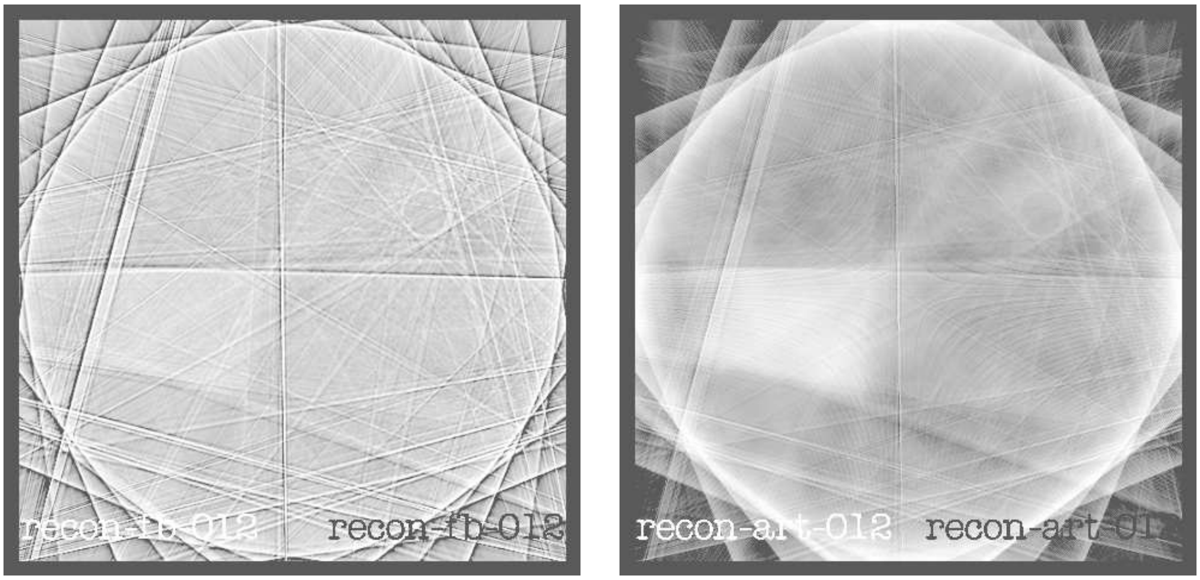

(a) (b)

Figure 6: Image reconstruction from 12 scouts. (a) Filtered Back-projection. (b) Algebraic Reconstruction (ART).

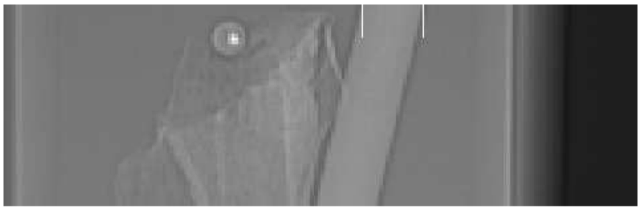

(a)

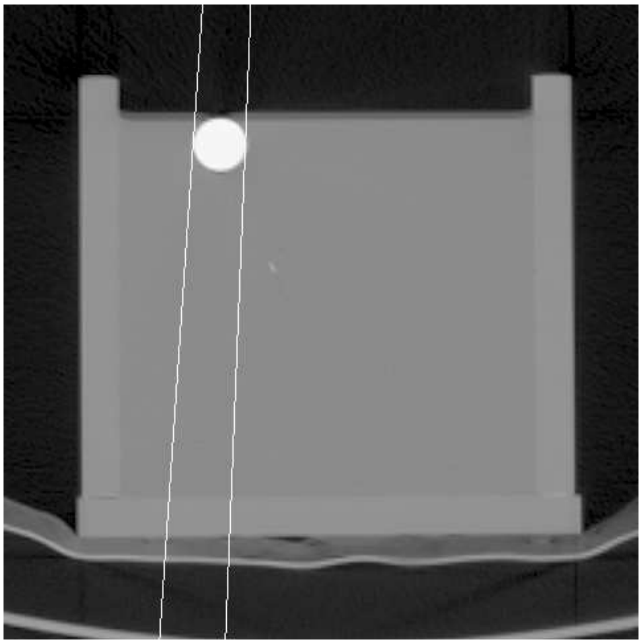

(b)

Figure 7: (a) A pair of scout edges. (b) The corresponding pair of image tangents.

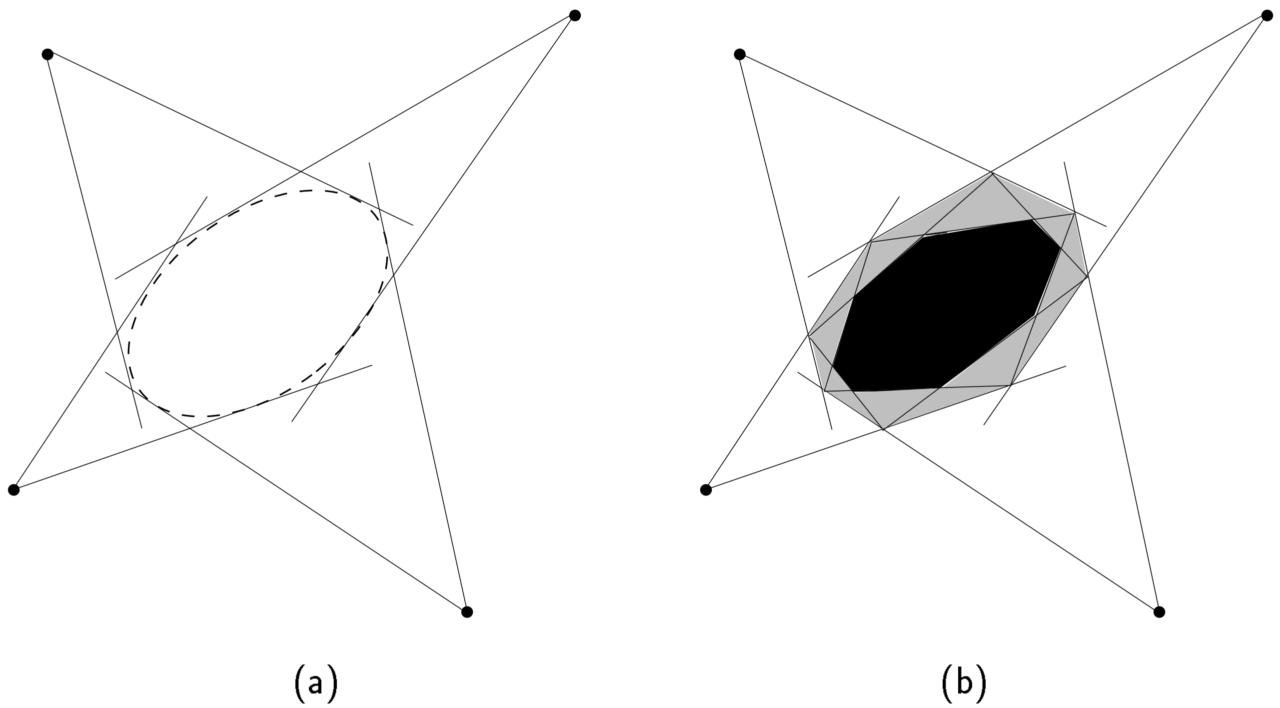

Figure 8: (a) An unknown convex shape with tangent lines. (b) Partitioning the plane based on these linear constraints.

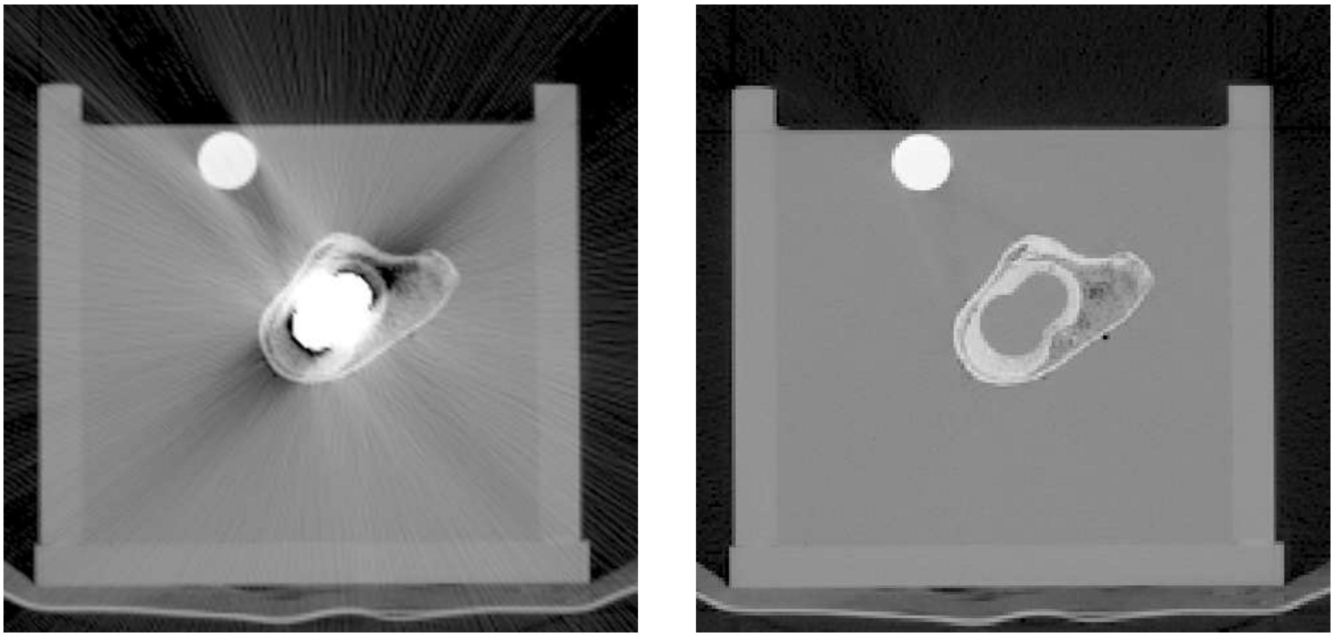

(a) (b)

Figure 9: The cadaver femur with the metal implant (a); and without it (b).

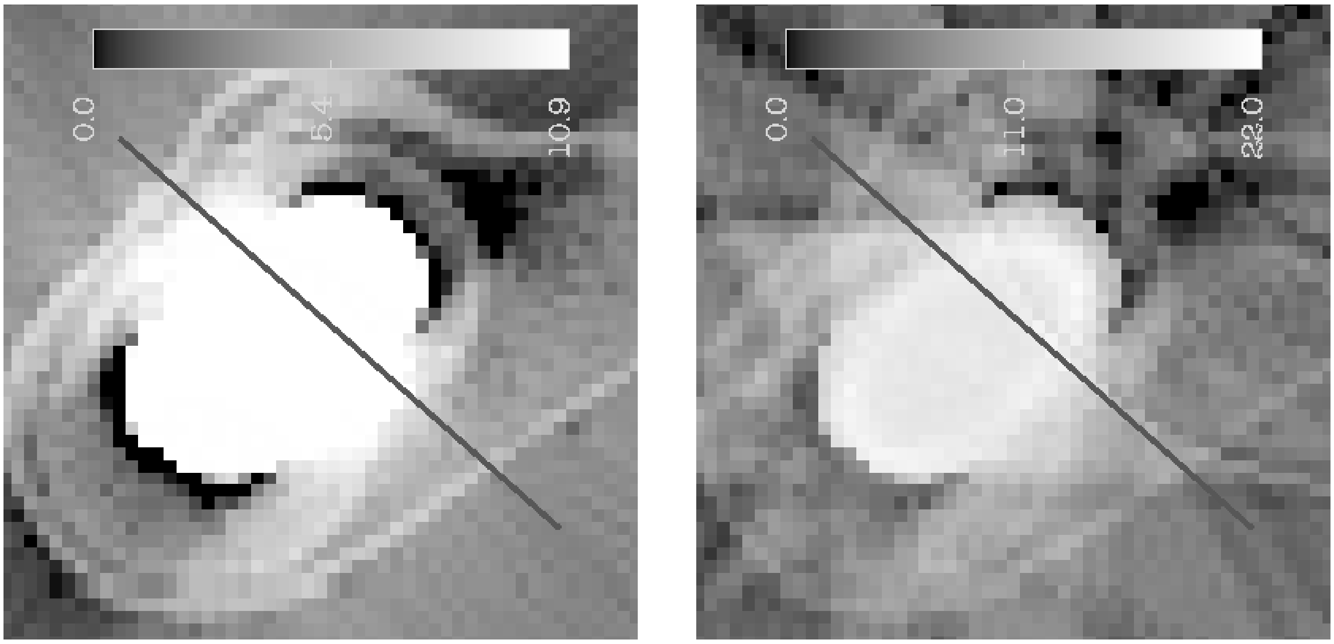

(a) (b)

Figure 10: Detail of CT image before (a) and after artifact reduction using MARCUS.

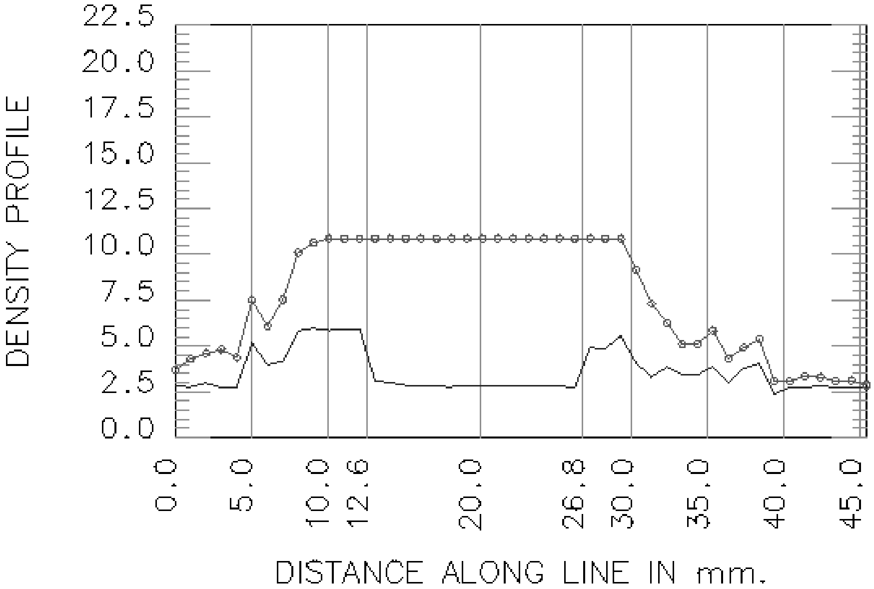

Figure 11: Density profile along line in Figure 10 (a).

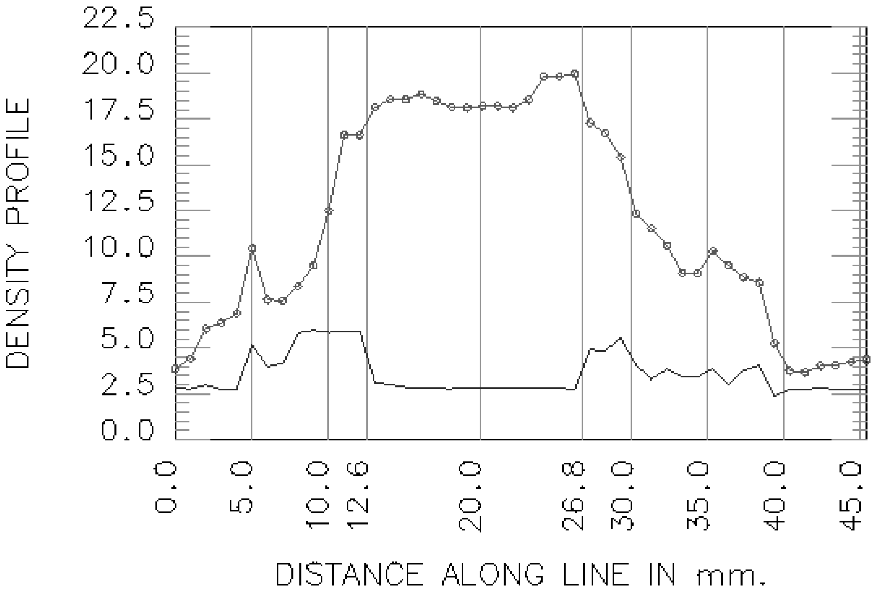

Figure 12: Density profile along line in Figure 10 (b).